MEGABIN 3D VERSUS CONVENTIONAL 3D METHODS WITH EXAMPLES FROM THE MICHIGAN BASIN

Norm Cooper, Mustagh Resources Ltd., Calgary, Alberta
Jim Egden, Union Gas Limited, London, Ontario

ABSTRACT

Two 3D programs were recorded in close proximity in Lambton County of the Michigan Basin by Union Gas Limited. The objectives were to image Silurian pinnacle reefs in a cost effective manner. One 3D employed conventional orthogonal techniques while the other employed the "MegaBin" method.

This paper reviews the design and characteristics of each method. The theory of the "MegaBin" method is explained. We briefly compare aspects of design, acquisition and processing. Samples of each survey are shown to demonstrate some differences in image quality and interpretability. Finally, we will summarize the cost effectiveness of each approach.

A DISCUSSION OF IDEAL SEISMIC IMAGING

The basic principle of reflection seismic is to generate an acoustic wavefront in the earth. This is usually accomplished by detonating dynamite charges buried a few meters below the surface or by using a machine that vibrates and shakes the earth with a controlled signal spanning a significant frequency range. Once introduced into the earth, the wavefront will expand spherically according to the acoustic velocity of the rocks in which it propagates.

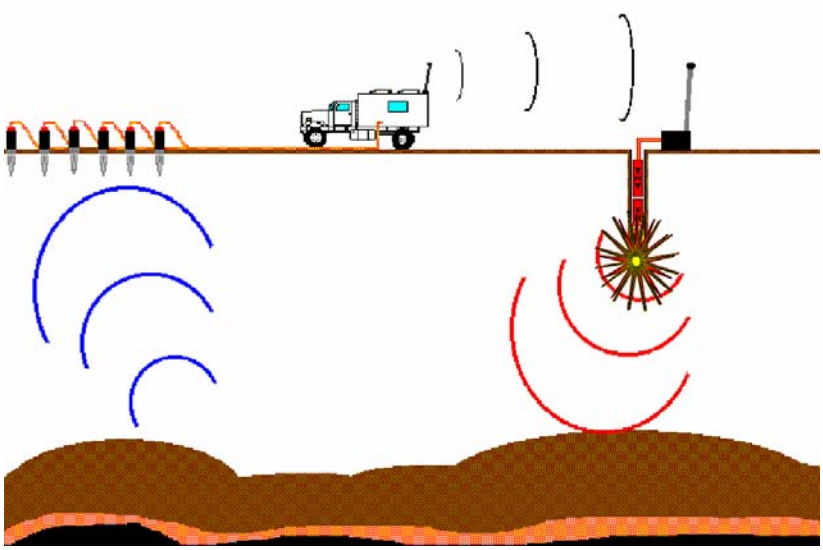

Figure 1
Fundamental seismic imaging.
We introduce an acoustic wave into the earth. As it expands and interacts with the earth, it becomes a complex wavefield, portions of which return to the surface during our seismic record. How frequently in time and space we choose to observe this returning wavefield (and how frequently we choose to inject it) is called *wavefield sampling*.

Irregularities in the subsurface will distort the developing wavefield. Each distinct boundary between rock layers of different types will cause the wavefront to bifurcate into reflected and transmitted elements. The wavefield becomes complex and is uniquely determined by the geologic changes within range of the seismic experiment. We record the wavefield at the surface where, during the time of our seismic record, portions of the wavefield return (see Figure 1). Our seismic record length varies from basin to basin and is usually not much longer than one second in the Michigan Basin.

The wavefield consists of continuous changes in time and space. By observing and recording these changes, we hope to reconstruct an image of the geologic features which distorted the wavefield to be just the way it is. This reconstruction process is the task of the data processors and interpreters. For reasons of economic and equipment limitations, we are not able to record the wavefield continuously at all points in time and space. The job of the program designers and acquisition contractors is to ensure that we record a sufficient subset of the full wavefield so that the processors and interpreters can do their part of the job.

Historically, we have recorded data in time at a sample interval of 1, 2 or 4 milliseconds. In the Michigan Basin, the most common sample rate today is 1 millisecond. This proves to be sufficient to record the frequencies of the wavefield that survive during our seismic experiment. We often find useable data from 10 Hz to 180 Hz. These frequencies should allow us to image features as small as 15 to 20 meters at the Silurian Guelph level. Therefore, 3D surveys are typically designed to yield bin sizes (stacked trace intervals) of 15 to 20 meters. This determines the basic spatial sample interval at the surface of 30 to 40 meters.

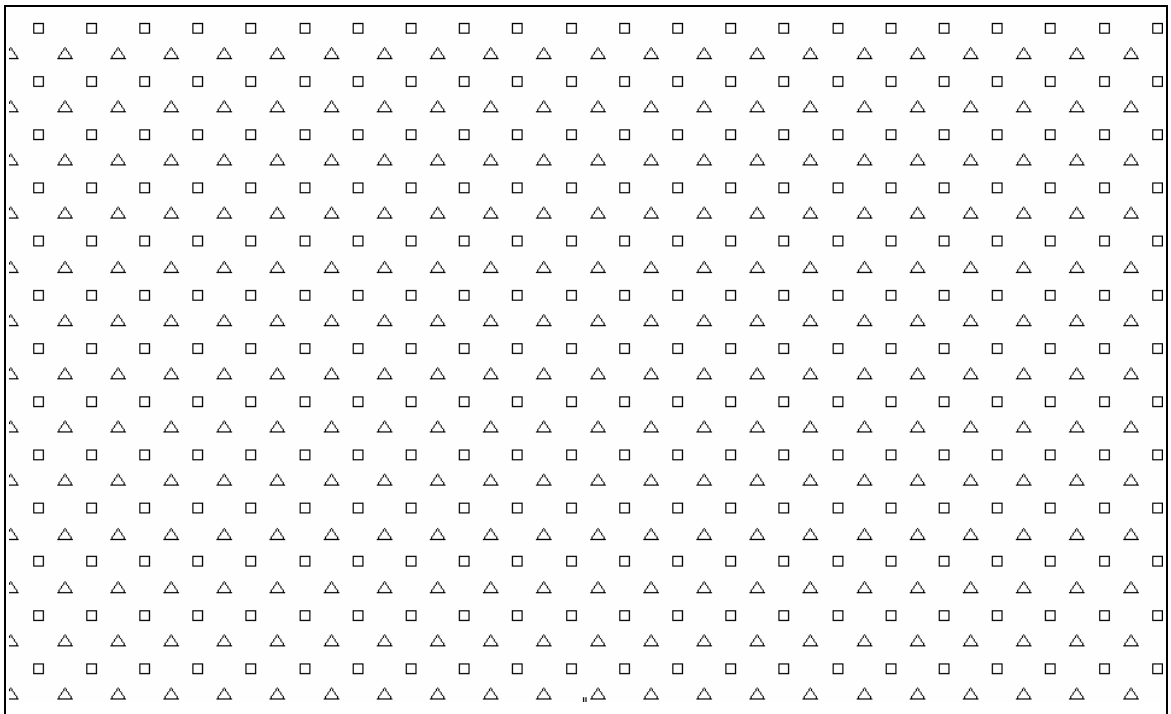

Figure 2
Diagram of a *"Full Wave Field Sampled"* 3D layout.
In this example the receivers (triangles) are 40 m apart along each line
and there is a line of receivers every 40 meters.
The sources (squares) are organized in the same pattern but offset from the receivers.

In order to fully sample the returning wavefield at such a spatial frequency, we should use a grid of

receivers with one trace being generated every 40 meters by 40 meters at the surface. In order to fully image the subsurface with sources from all angles and directions, we should use a grid of source points generating wavefronts every 40 meters by 40 meters. In order to optimize the statistical diversity of the seismic experiment we should offset the source and receiver grid. Figure 2 shows such an arrangement.

For each shot that is generated, we must record traces within the maximum useful offset as determined by our target depth and the overlying velocity structure. For the examples considered in this study, the maximum useable offset for the Silurian Guelph reefs is about 450 meters.

If we record all of the shots in the grid described in figure 2 at different times, we will produce overlapping images of the subsurface which will strengthen the image quality. The amount of overlap is called the "fold" of the survey. For the grid in figure 2, we can calculate the fold in each 20 m by 20 m subsurface bin. This is displayed in figure 3 where we observe the nominal fold to be 100 (except at the edges of the survey where imaging statistics are deficient). So each subsurface area of 20 x 20 meters will be imaged by 100 different traces generated by different source-receiver combinations. What a wonderful level of statistical sampling … if only we could afford it !

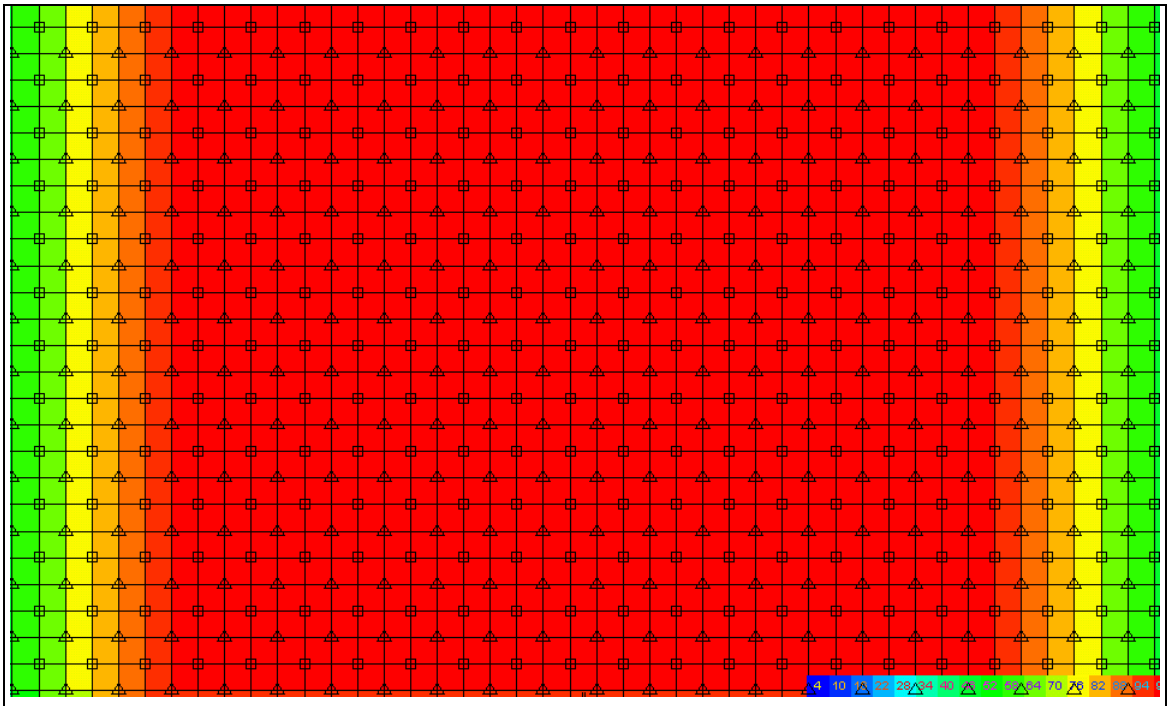

Figure 3
Full Wavefield Sampling – fold to 450 meter offsets.
The edges of the survey drop below 50 fold, but all bins in the center are 98 fold.

The above discussion details a design known as "Full Wavefield Sampling". Given spatial and temporal bandwidth limitations, our minimum realizable sample intervals are defined. Ideally, we would like to sample our data at these intervals in all domains. Unfortunately, this would place high demands on equipment utilisation, landowner impact and program cost. Let us study two different compromises to full wavefield sampling. One is typical of "orthogonal" 3D designs often used in the Michigan Basin, the other is the "megabin" approach developed by PanCanadian Petroleums in Alberta.

ONE ALTERNATIVE – THE MEGABIN DESIGN

Let's examine the impact on the fold if we start decimating the full wavefield sampled 3D. First, let's remove every second line of source points in the north-south direction (see figure 4). Note that the fold drops to a peak of 50 and the level of fold alternates slightly in north south stripes. This is called "striping" or "banding" by 3D designers and can be destructive to the image quality if exaggerated. At this level it is absolutely no problem as variations are small compared to the median fold.

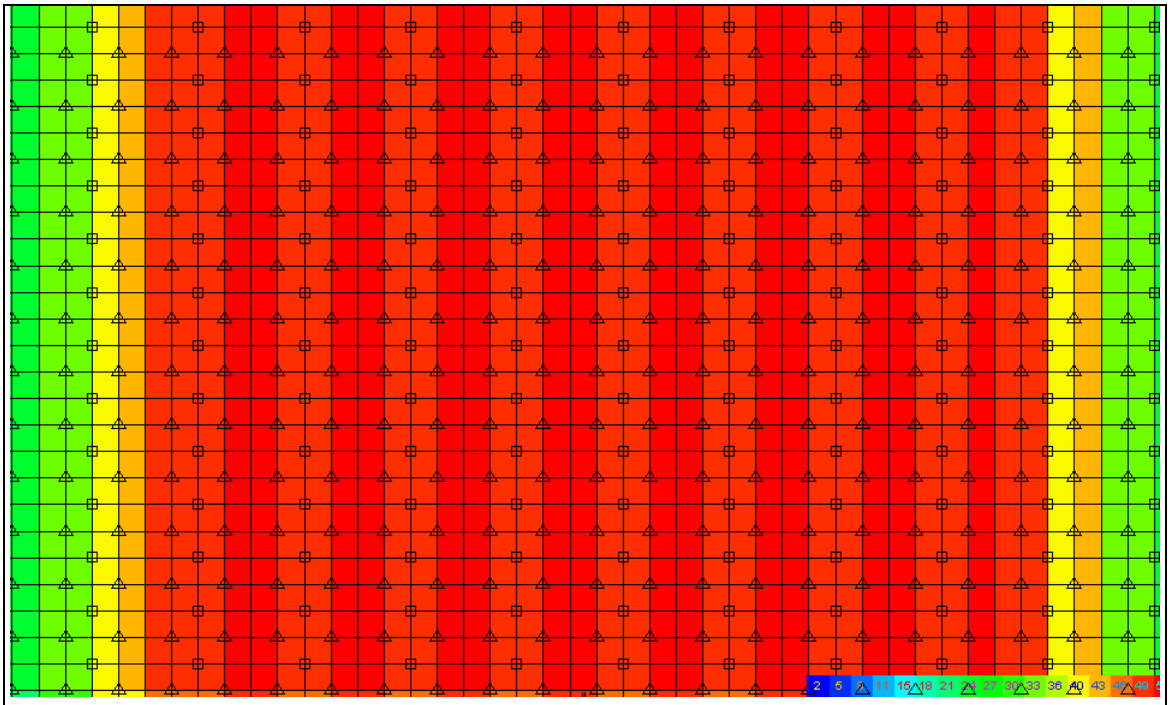

Figure 4
½ Source Sampling – fold to 450 meter offsets.
Every second north-south source line has been eliminated. Full fold varies between 47 and 51.

Figure 5 illustrates the results of further decimation where we have removed every second line of receivers in the north-south direction. Notice that the fold in imaged bins remains the same, but now we fail to illuminate every second column of in-line bins. This is characteristic of the "megabin" method and does not represent any significant problem. The greatest danger is the aliasing of the migration process. Therefore, prior to migration, the data set is interpolated to fill the missing columns. Generally, a robust F-X domain interpolation operator is used (Spitz, 1991 or Porsani, 1999). This provides meaningful trace data (to the extent that the number of dips does not exceed the number of lines in the design window). After migration, both interpolated and original recorded data are mixed and moved within the migration aperture. Every post-migration trace consists of a mixture of both original and interpolated traces.

Figure 6 shows the impact of deleting one half of the remaining source points. Of course, fold is reduced to a maximum redundancy of 25 traces per bin and there is still a mild heterogeneity from one column of bins to the next. This is of no significance provided the median remains above 10 fold. Figure 7 is a minor adjustment where the source points are moved from their staggered position to a location in line with the receivers. This enables the program to be recorded from a single set of parallel lines and minimizes landowner impact.

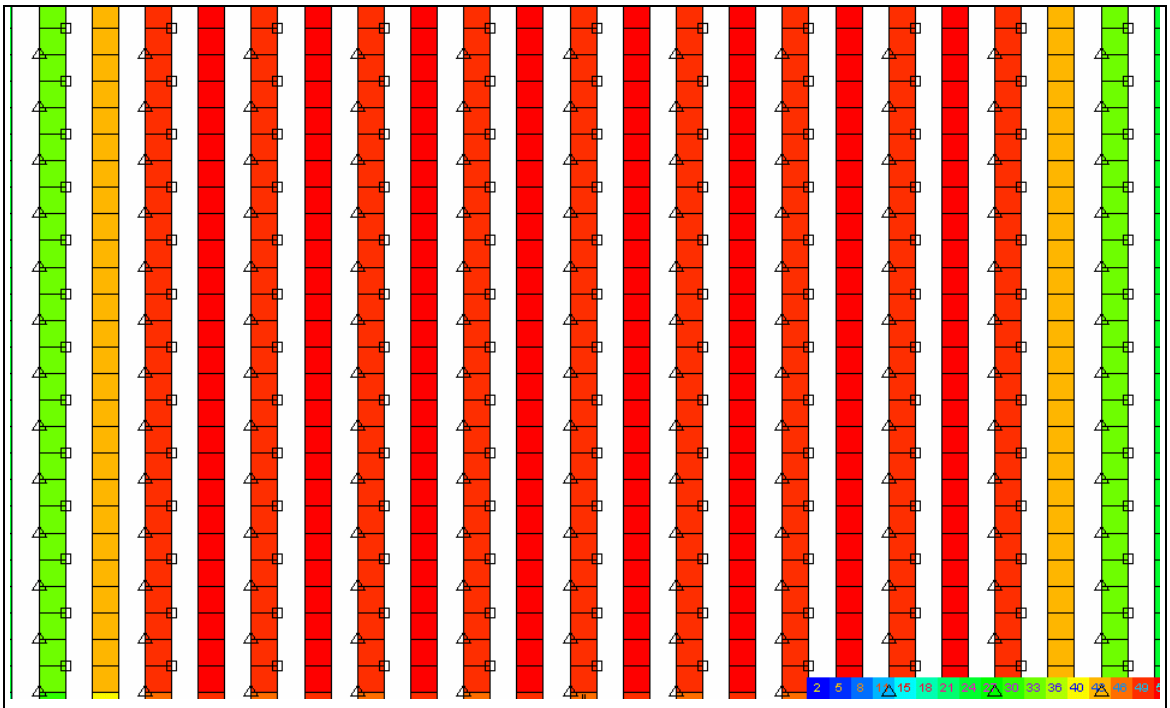

Figure 5
½ Source ½ Receiver Sampling – fold to 450 meter offsets.
Full fold varies between 47 and 51 in imaged bins and zero in alternate bins.

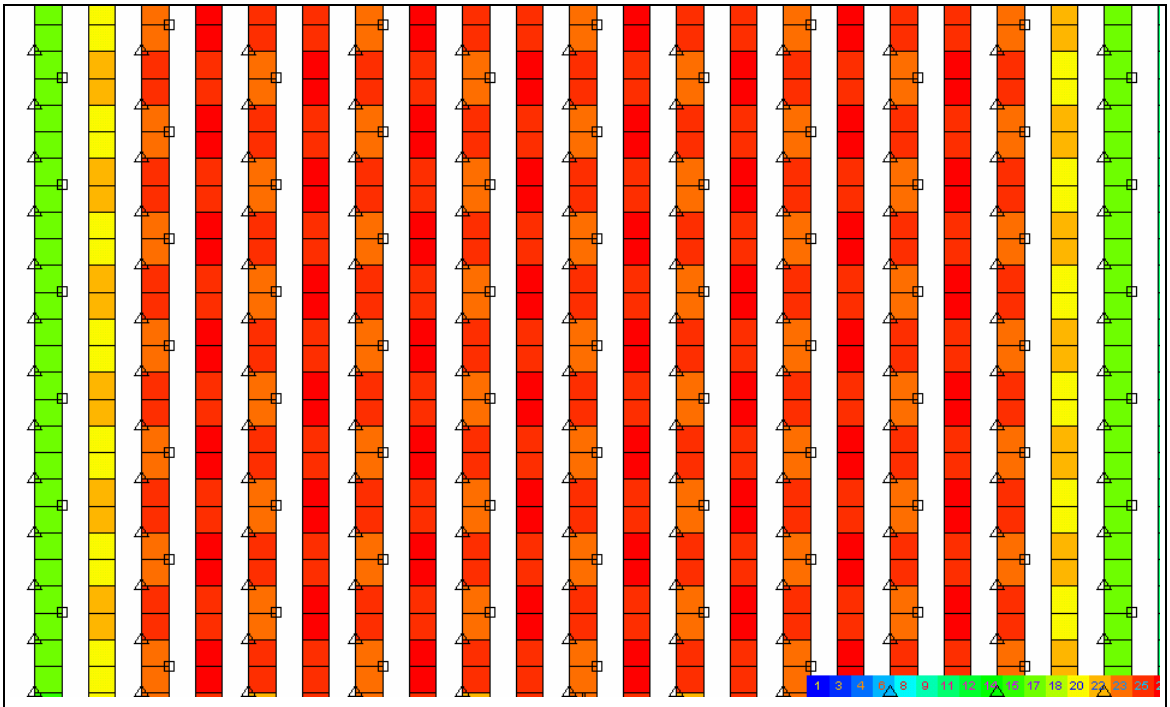

Figure 6
¼ Source ½ Receiver Sampling – fold to 450 meter offsets.
Fold is 25 and 26 between surface lines; 23 and 24 below surface lines.

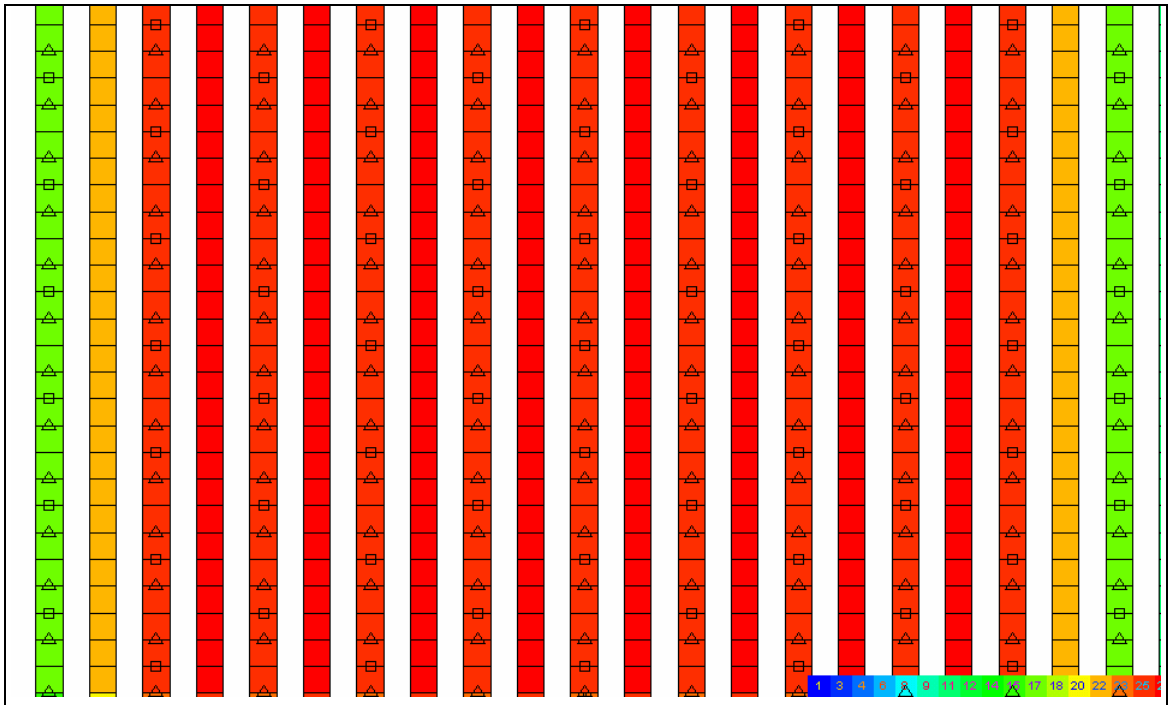

Figure 7
Megabin – fold to 450 meter offsets.
Fold is 26 between surface lines; 24 and 25 below surface lines.

Figure 7 shows the design developed by PanCanadian Petroleums known as "megabin". It is one approximation to full wavefield sampling where only half the required number of receivers are used. This reduces the line density and lowers landowner impact and survey cost. The penalty paid in image value is that every second bin in the crossline direction remains un-imaged. This deficiency is compensated by applying a spatial interpolation before migration. The sources are sparsely sampled by a factor of one half in both inline and crossline directions. The effect is to reduce fold in imaged bins and reduce some offset statistics (to be demonstrated later). The crossline decimation is necessary to be consistent with the receiver line decimation and to enable the reduction of line spacing. The inline decimation is not entirely necessary, but for larger fold 3D's is not significantly detrimental to image quality and this decimation helps reduce costs (at least in dynamite surveys). It should be noted that vibroseis megabin 3D's should still occupy every source point but perhaps use one half of the expected vertical stack effort (half the number of sweeps).

Note that with sources and receivers falling on coincident lines, it is not necessary to have orthogonal lines connecting sources. This savings in linear kilometers of line to be produced (as well as reduced permitting and damages) makes the megabin very cost effective in areas where dense grid 3D's are being considered.

ANOTHER ALTERNATIVE – THE ORTHOGONAL DESIGN

Let's start again with the full wavefield sampled 3D pictured in figures 2 and 3. Only this time (for consistency with later examples, we will sample the surface in 30 meter intervals (in both source and receiver domains). This will yield subsurface sampling in 15 meter bins. The fold diagram (again limited to the useful offsets of 450 meters at the Silurian Guelph level) is shown in figure 8. This time (due to the tighter grid density), the nominal fold is about 176.

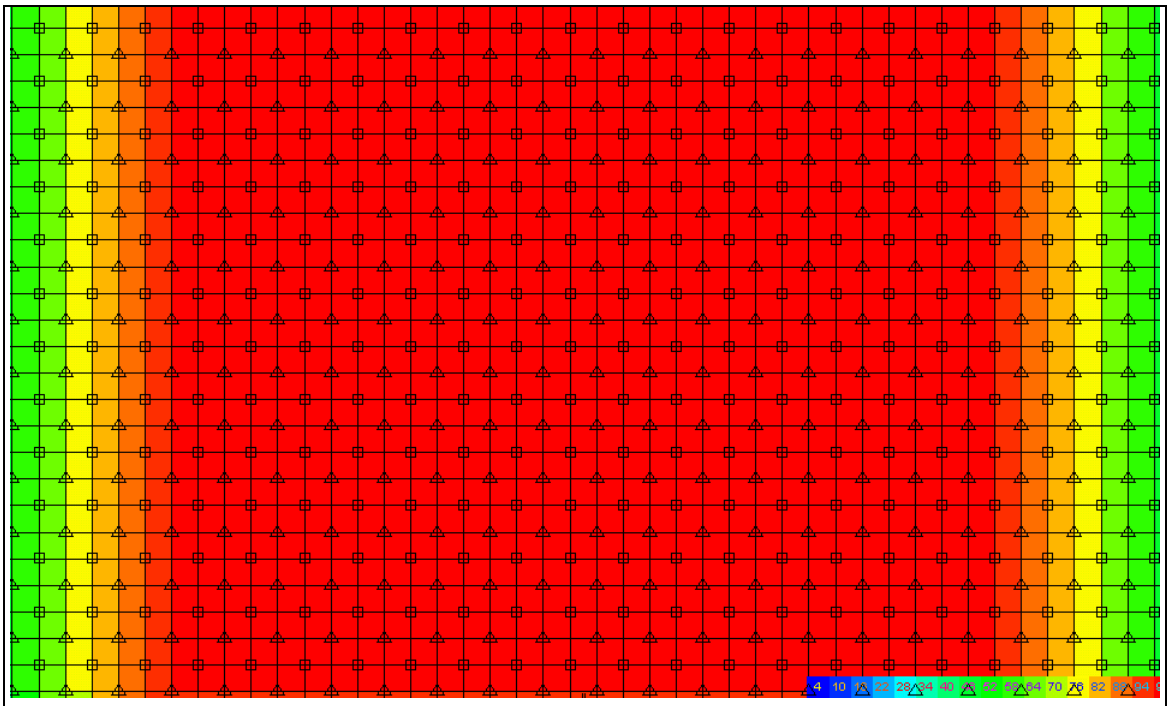

Figure 8
Full Wavefield Sampling – fold to 450 meter offsets.
The edges of the survey drop below 50 fold, but all bins in the center are 179 fold.

The fold diagram in figure 9 results when we eliminate two out of three source lines in the east-west direction. In this decimation, we are left with east-west lines of source points and the source line spacing is 90 meters. The resulting fold is reduced to one third (on average) and now appears to vary between 58 and 62. This represents a slight heterogeneity and shows east-west banding. However, with the high level of average fold, this will not adversely effect the data.

We further decimate the data in figure 10 by eliminating half the receivers (every second north-south line). We now have an orthogonal grid of data with a 90 meter source line spacing and 60 meter receiver line spacing. Notice that the orthogonal arrangement of sources and receivers ensures that every bin will be imaged with original traces. However, this decimation reduces fold by a factor of two (now ranging between 28 and 31 fold). We also begin to notice a checker board pattern of fold variation. With an average fold near 30, this variation only represents a plus or minus 6 percent fluctuation and we are not yet concerned about geometric imprinting in the data.

Figure 9
Source 90 Receiver 30 – fold to 450 meter offsets.
Full fold varies from 58 (between source lines) to 61 (below source lines).

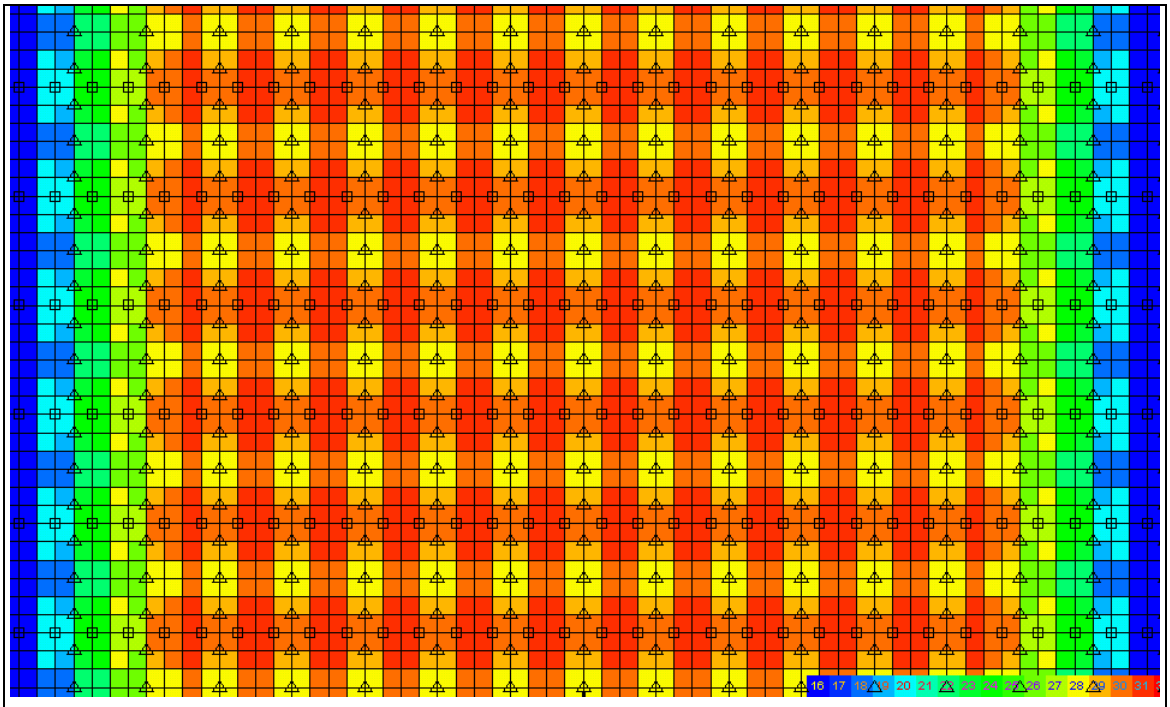

Figure 10
Source 90 Receiver 60 – fold to 450 meter offsets.
Full fold varies from 28 to 31.

Figure 11 represents one more level of decimation where we have removed half of the remaining receiver lines to produce an orthogonal grid with source lines spaced 90 meters apart and receiver lines spaced 120 meters apart. The fold now varies from 12 to 16 (14 plus or minus 2). This is a 14 percent variation around the median fold and, in our experience, may be sufficient to generate a mild amount of geometric imprinting.

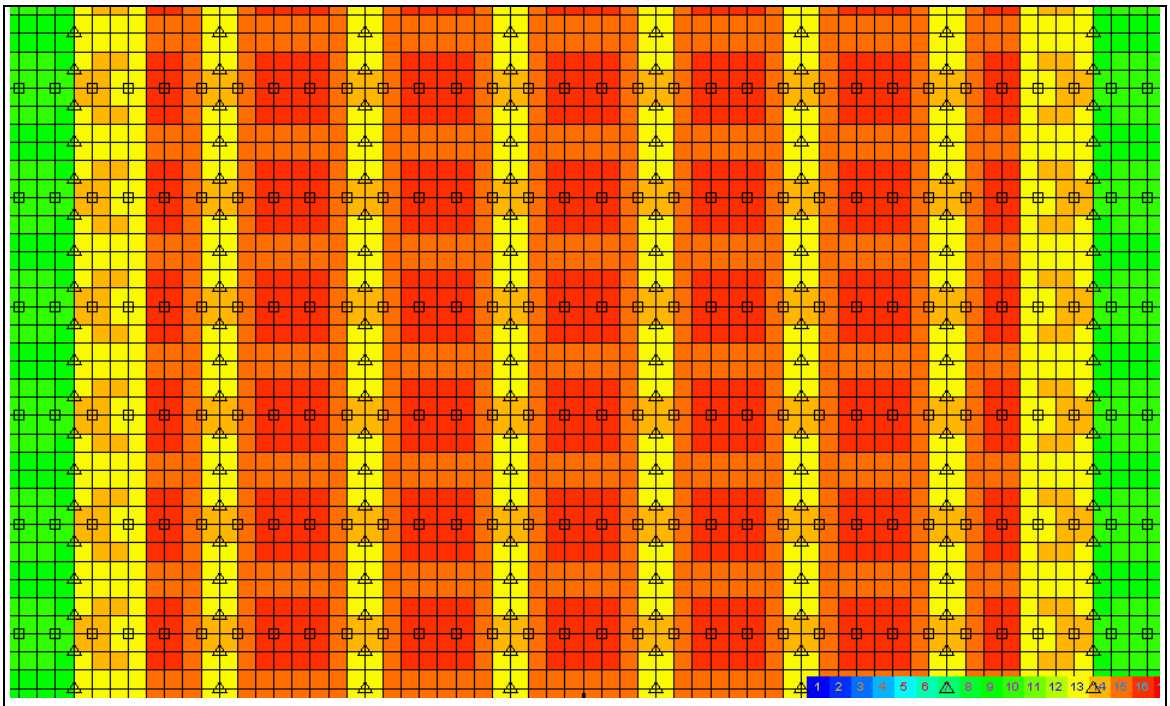

Figure 11
Source 90 Receiver 120 – fold to 450 meter offsets.
Full fold varies from 13 (below receiver lines) to 16 (darker colors).

Of course, fold is not the most important statistic to concern ourselves with. In the following series of figures, we will compare the offset distribution of an ideal (full wavefield sampled) 3D to the megabin approximation and the tight grid orthogonal.

Offset distribution plots indicate the source-receiver offset characteristics of the collection of traces that image each bin. In figure 12, each bin is imaged by 176 traces. Some of these traces were generated by source-receiver pairs in close proximity to each other (near offsets) and are represented by very short vertical line segments located at the left of each bin. Long offset traces are represented by longer vertical line segments positioned at the right side of each bin. A bin that is imaged by a broad variety of offsets will appear as a filled triangle. The color (or grey shade) of each vertical line segment indicates statistical redundancy. That is, some offset ranges are repeated by more than one trace. Fold generated by statistically diverse offset distribution is constructive for enhancing signal to noise ratio in the stack process. Redundant observations contribute much less value in the stack.

The full wavefield sampled survey shown in figure 12 has sampled at least one trace in every possible offset range (n ± ½ × bin size in meters [for n=1 to 30 representing 15 to 450 m of offset]) except for the offset at 2 ± ½ × 15 m. Note that we collect traces in offset ranges centered on integer multiples (n) of our bin size. Each vertical bar represents one value of n. The left most (short) bar represents n=1 or an offset of 0.5 to 1.5 bin sizes. The next bar represents 1.5 to 2.5 bin sizes (n=2). The last bar represents the maximum useable offset (n = Xmax / bin size).

In the middle and far offsets, there is a high level of redundancy. This is a result of wide aperture recording where we expect 5/9 of our traces to come from the far third of the offset range and only 1/9 to come from the near third.

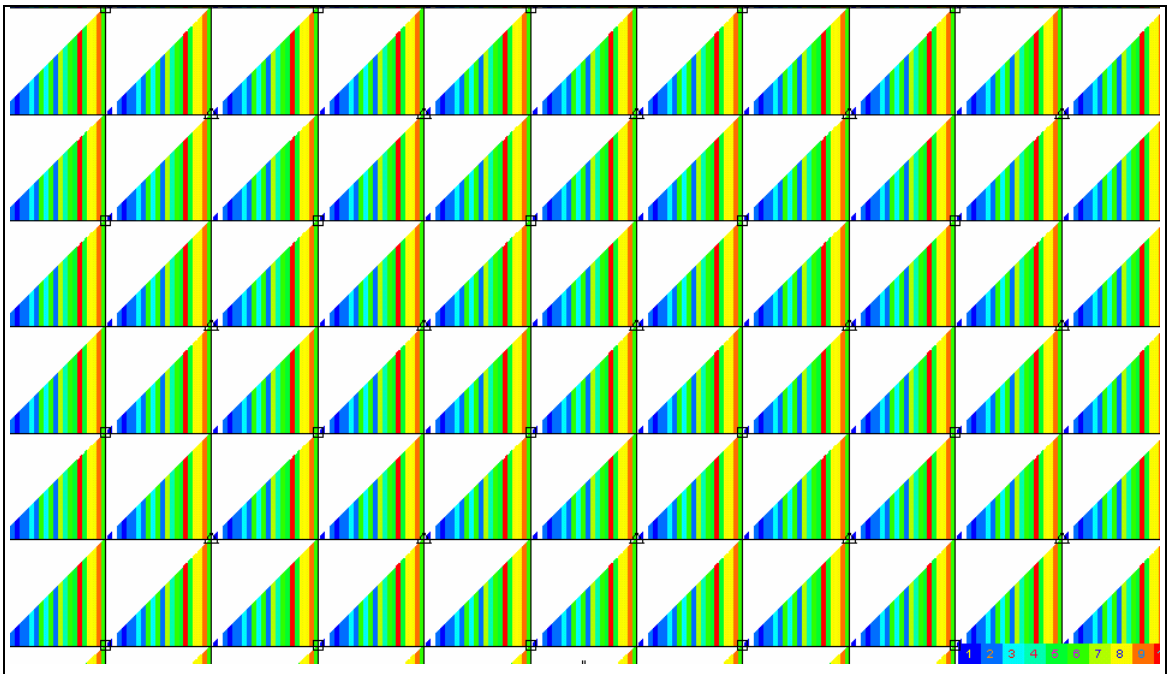

Figure 12
Full Wavefield Sampling – offset detail.
Redundancy ranges from 0 to 10 observations per offset.

Figure 13 shows the offset distribution resulting from the megabin model. Note that the bins between surface lines are quite well imaged, while the bins underlying the surface lines demonstrate a few offset deficiencies. Any time we choose not to record full wavefield sampling, we must sacrifice some of our statistical sampling. In this model, the patterns occur in pairs due to the sparse source sampling along the surface lines. These bins would be better sampled and uniform if the source interval matched the receiver interval (an affordable strategy for vibroseis programs).

Figure 14 is the offset distribution resulting from the orthogonal model. Notice the significant bin to bin heterogeneity. Most bins have significant deficiencies (large gaps of missing offsets). We concern ourselves with the "clumpiness" of offset distributions. There are small regions of offsets densely sampled and other regions very sparsely sampled. The character of this "clumpiness" varies greatly from one bin to the next.

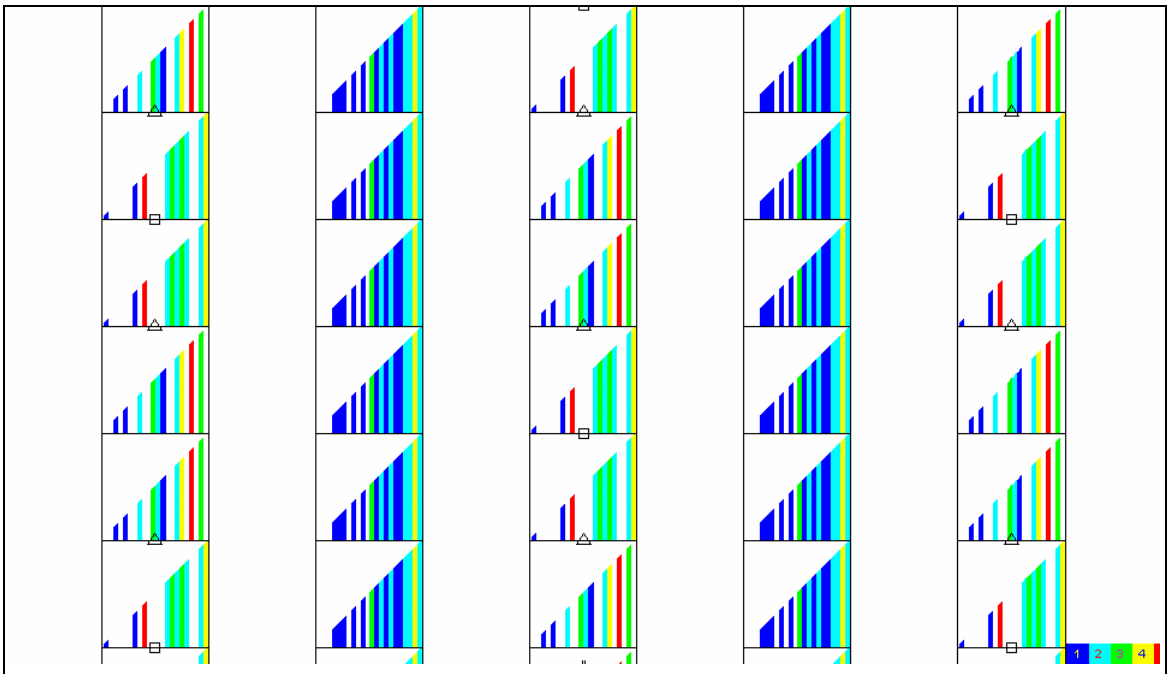

Figure 13
Megabin – offset detail.
Redundancy ranges from 0 to 5 observations per offset.

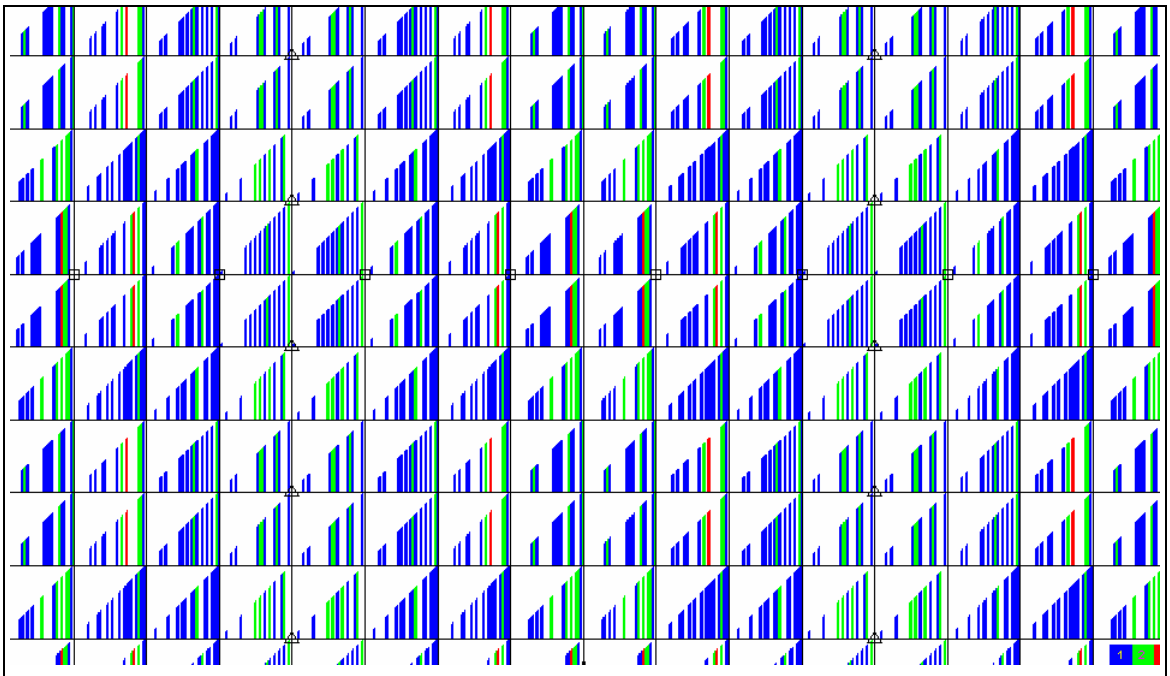

Figure 14
Source 90 Receiver 120 – offset detail.
Redundancy ranges from 0 to 3 observations per offset.

In order to study the patterns of "clumpiness" on a larger scale, we have developed a "homogeneity" plot. Figure 15 shows the offset homogeneity for the full wavefield sampled model. For each bin, we calculate the distribution of traces as a function of offset squared (to account for wide aperture recording). We then tabulate the differences in offset between each successive offset in a sorted list. A bin containing well distributed offsets will have a small standard deviation in these differences. A "clumpy" distribution will yield a larger standard deviation. The standard deviation of the delta-offset-squared list represents a single number which can be plotted for each bin and represents the uniformity of offset sampling in each bin. A small standard deviation is good (less than 4 percent), values from 4 to 8 represent fair sampling, and values in excess of 8 to 10 percent represent quite poor offset sampling. Full wavefield sampling shows all full-fold bins with about 1 percent standard deviation. This represents excellent offset statistics.

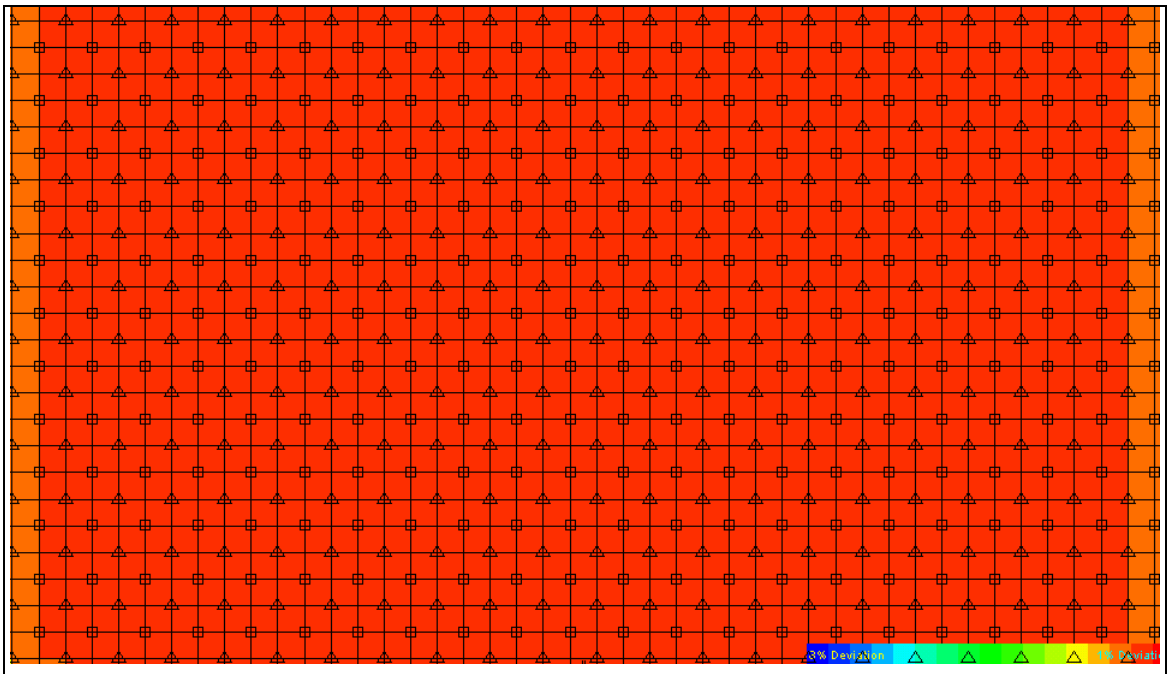

Figure 15
Full Wavefield Sampling – offset homogeneity.
Standard deviation in full fold bins is 1.34 percent.

Figure 16 is the offset homogeneity plot for the megabin model. The bins between surface lines exhibit standard deviations of about 2 percent while the bins below the surface lines vary in the 5 to 6 percent range. This survey is very well sampled in offset.

Figure 17 is the offset homogeneity for the orthogonal model. About half the bins exhibit more than 6 percent standard deviation. This is not very bad by standards for surveys in the western Canadian basin, but is still substantially inferior to the megabin model.

Many other statistical measures can be compared for these two models (largest offset gaps, azimuth distribution, azimuth homogeneity, largest azimuth gaps). However, we will reserve these comparisons for the real data examples that follow.

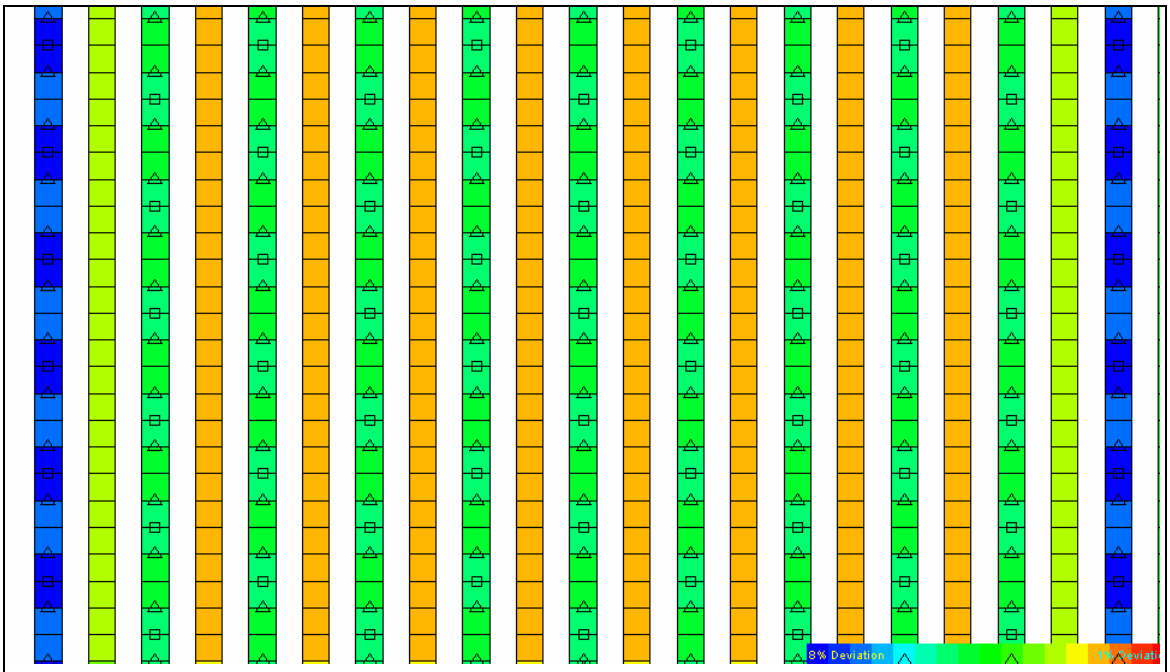

Figure 16
Megabin – offset homogeneity.
Standard deviation is 2.52 % between surface lines and 5.09 or 5.37 below surface lines.

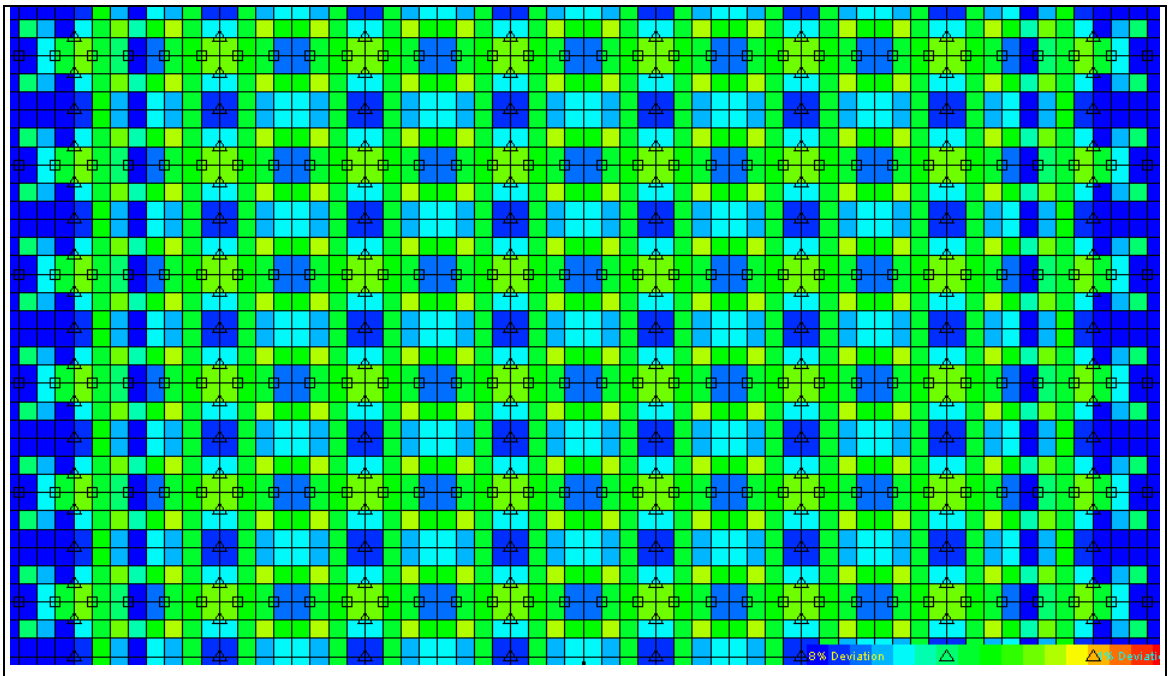

Figure 17
Source 90 Receiver 120 – offset homogeneity.
Standard deviation in full fold area varies from 3.3 (lighter colors) to 7.41 (darker colors).

STATISTICAL EVALUATION OF CASE HISTORIES

Figure 18 shows the relative location of two 3D surveys conducted in SW Ontario. The survey to the southeast is known as Bentpath East and was recorded in September of 1997. The survey to the northwest is called Booth Creek and was recorded in the summer of 1998. The centers of the two surveys are less than 2 kilometers apart.

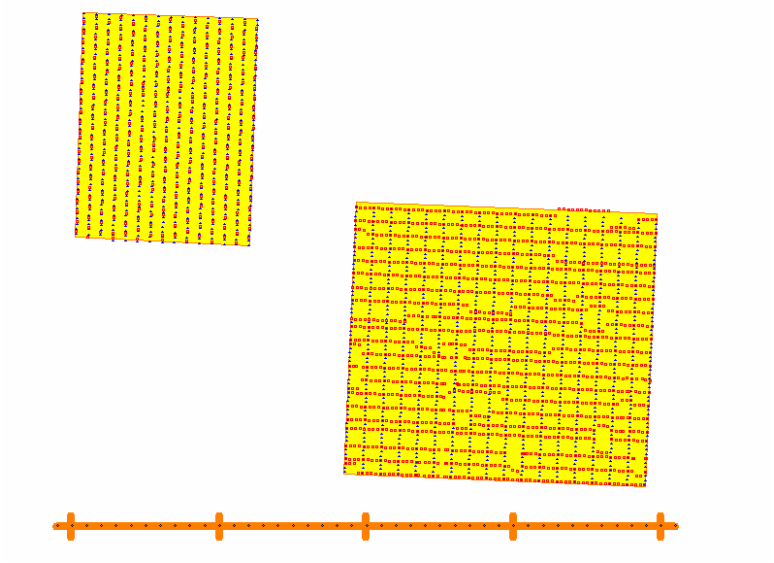

Figure 18
Booth Creek versus Bentpath East – basic grids and relative location.
Major divisions on scale are separated by 1000 meters.

The following table summarizes information and parameters for the two surveys:

	Booth Creek	**Bentpath East**
Design Consultant	Mustagh	Geo-X
Acquisition Contractor	Can Geo	Can Geo
Date Acquired	Summer, 1998	September, 1997
Model Style	MegaBin	Orthogonal
Size	1.530 x 1.176 km	2.040 x 1.800 km
Area	1.8 km^2	3.67 km^2
Recording System	Das – 1 ms sample rate	Das – 1 ms sample rate
Receiver / Source Interval	34 x 68 m	30 x 30 m
Receiver / Source Line Spacing	84 x 84 m	120 x 90 m
Natural Bin Size	17 x 42 m	15 x 15 m
Processed Bin Size	17 x 21 m	15 x 15 m
Patch (lines and stations)	12 x 34 (double shot)	16 x 36 (double shot)
Patch Size	1008 x 1156 m	1920 x 1080 m
Receiver Points	689 (383 per km^2)	1098 (299 per km^2)
Source Points	338 (188 per km^2)	1451 (395 per km^2)
Linear Receiver / Source km	22.950	32.400 + 42.840
Linear kms per km^2 – actual	12.755	20.490
Linear kms per km^2 – theoretical	11.905	19.444

Figure 19 compares the fold in natural bins for the two surveys. Note that the natural bins for Booth Creek are quite large (hence the name "MegaBin"). However, this data will be gathered in half size bins (as in figure 20), leaving every second bin empty. A robust F-X domain interpolator is used to infill the empty bins prior to migration. In figure 19 the fold scales are different for the two surveys (2-34 and 1-17). In figure 20 the figures share a common fold scale (13-29).

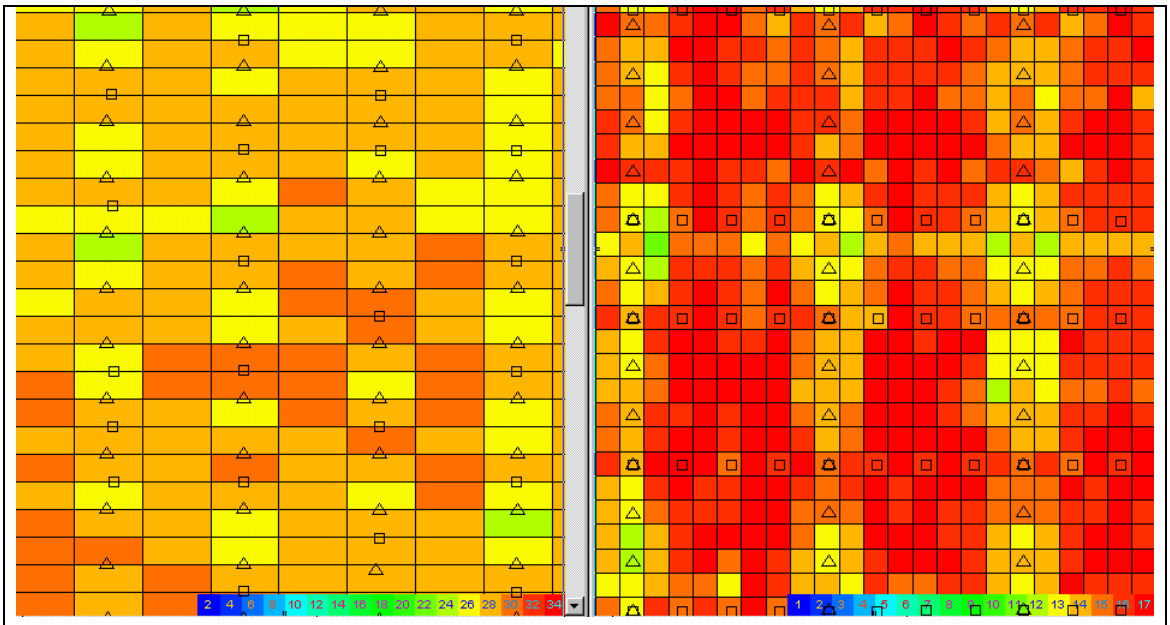

Figure 19
Booth versus Bentpath fold in natural bins.
Booth varies from 24 to 31 fold; Bentpath varies from 11 to 20 fold.

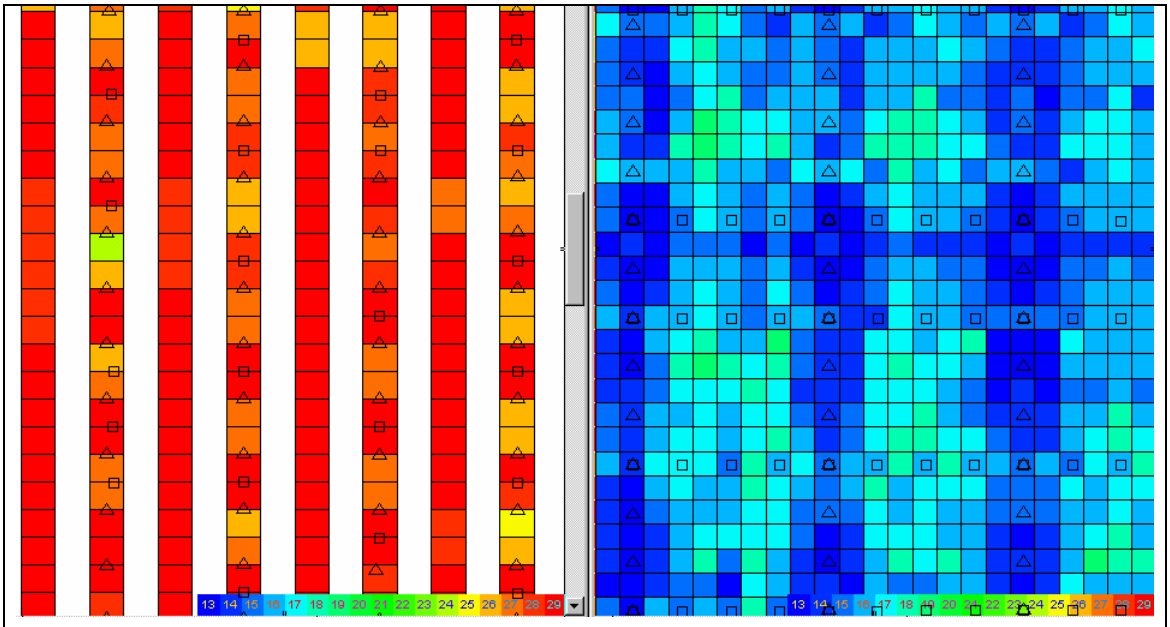

Figure 20
Booth versus Bentpath fold in processed bins.

Figure 21 compares the offset distribution for the two surveys. Note the greater deficiencies in the orthogonal design. Figure 22 highlights the worst case deficiency (or "gap") for each bin. The orthogonal survey varies from 67 to 180 m with a significant number of large gaps and great variation from bin to bin. The megabin design is more uniform with most of the gaps from 82 to 119 meters.

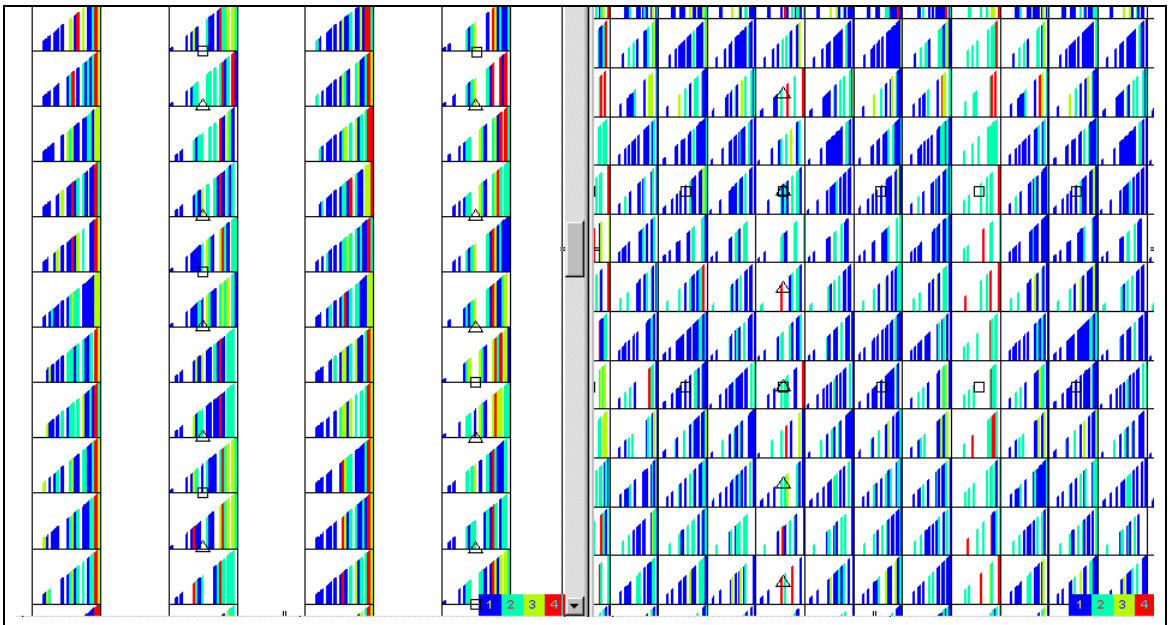

Figure 21
Booth versus Bentpath offset distribution.
Note the bin to bin uniformity of the MegaBin design.

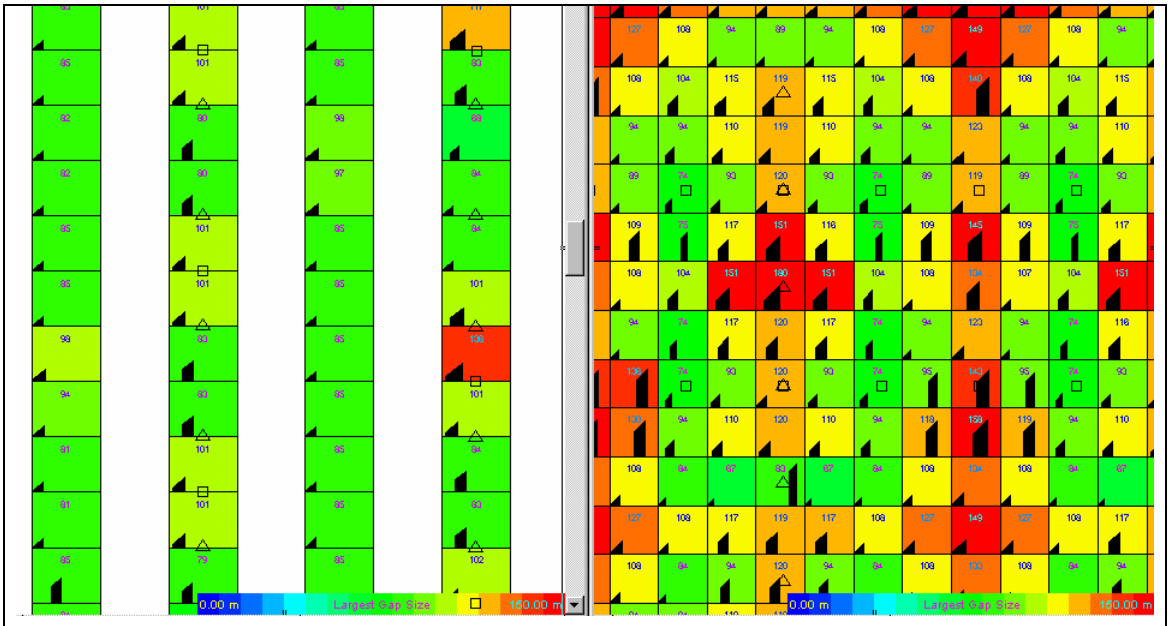

Figure 22
Booth versus Bentpath largest offset gap.

In figure 23 we have presented the offset homogeneity plot for the two surveys. Notice that the megabin survey yields much more uniform offset sampling in all bins. Homogeneous offset sampling is very important to stacked data quality, the consistency of multiple suppression and the stability of wavelet phase and amplitude.

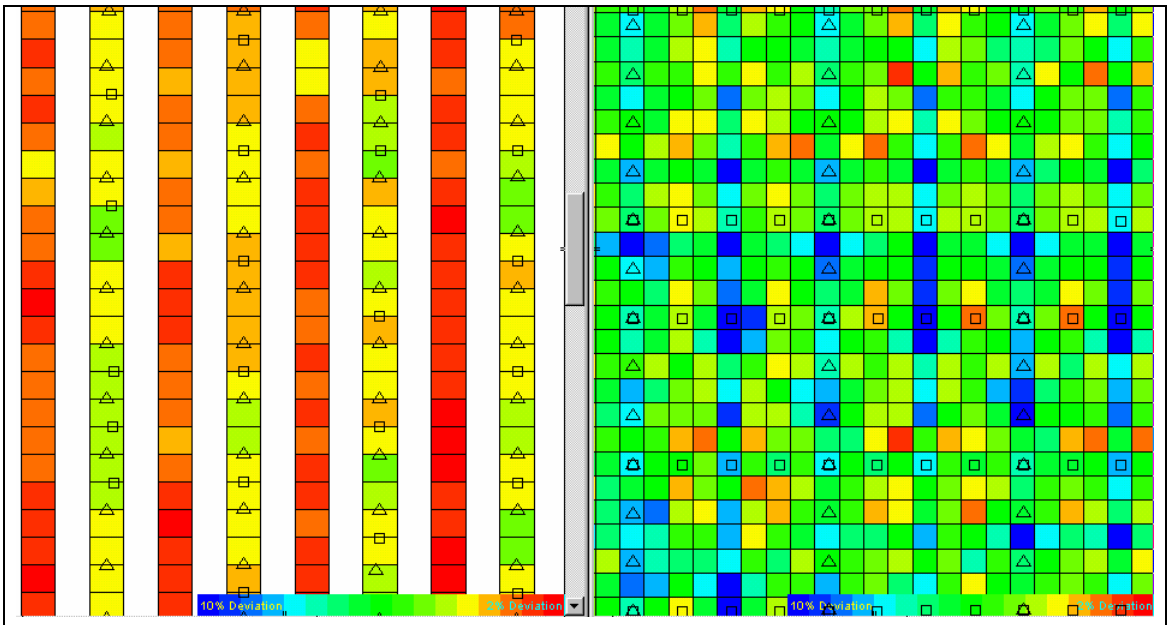

Figure 23
Booth versus Bentpath offset homogeneity.
Booth ranges from 2.3 to 4.7 %; Bentpath ranges from 2.5 to 11.3 % standard deviation.

Another important statistic of interest to 3D designers and processors is azimuth distribution. Image quality is enhanced if each stacked trace is the average of observations of the subsurface reflection from many different angles. Figure 24 shows the source-receiver alignment for all of the traces contributing to each subsurface bin. We refer to this as a "spider" diagram. The length of each leg of the spider is proportional to the source-receiver offset for that trace. A well sampled survey will exhibit bin to bin consistency in the spider plot and each bin will have a spider with legs of different lengths pointing in all different directions.

In each bin, we can sort the contributing traces by azimuth. Then we calculate the difference in azimuth between adjacent traces. Figure 25 shows a plot of the largest such angle for each bin. This "largest azimuth gap" indicates the worst occurrence of deficient azimuths of imaging for each stacked trace. The higher fold of the megabin design helps reduce the largest gap in azimuth. The density of the sampling stabilizes the bin to bin variation.

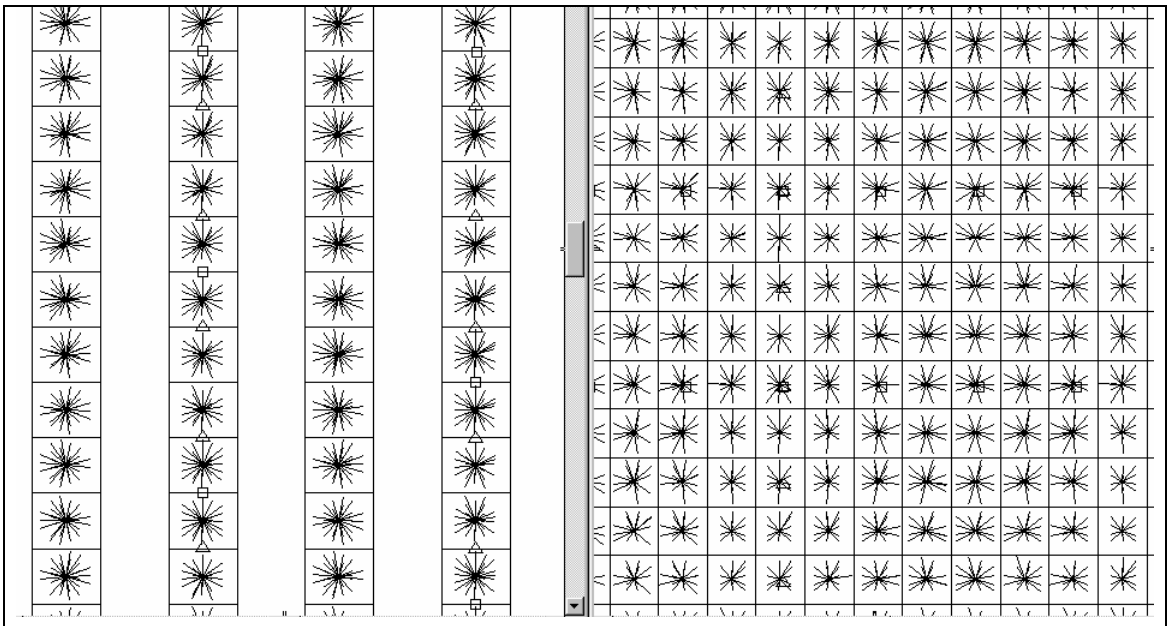

Figure 24
Booth versus Bentpath azimuth distribution.
Note the more consistent appearance of the megabin distribution.

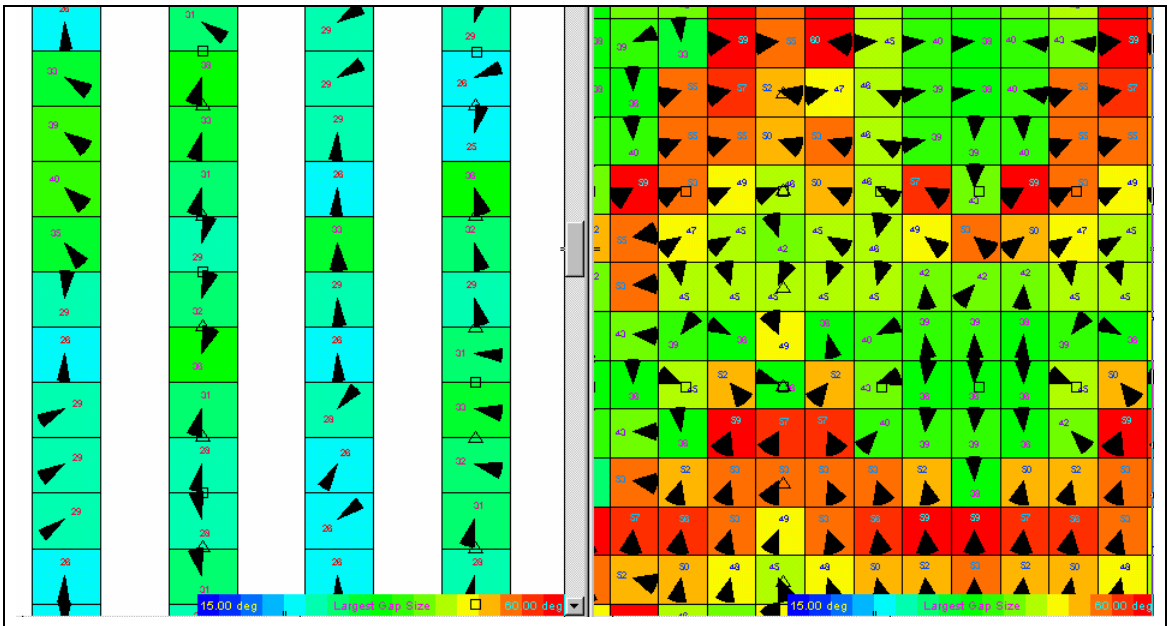

Figure 25
Booth versus Bentpath largest azimuth gap.
The orthogonal design not only has larger gaps, but they are more erratic in azimuth from bin to bin.
Booth varies from 26 to 40 degrees; Bentpath varies from 38 to 59 degrees.

If we use the same list of delta-azimuths, we can measure the standard deviation of the distribution for each bin . This will provide a single number that can be associated with the azimuth homogeneity of each bin. A low standard deviation means that azimuths are uniformly sampled. A higher standard deviation reflects more heterogeneity in azimuth distribution within each bin.

Figure 26 shows the azimuth homogeneity for the subject surveys. Homogeneous values (small values of standard deviation) indicate a stacked trace resulting from the average of well sampled raypaths. Consistency of color from one bin to the next indicates stability from trace to trace in the stacked data volume.

Note that the strength of the standard deviation is not influenced by fold. In other words, 6 traces well distributed with 60 degrees between each trace will provide a zero standard deviation the same as 12 traces well distributed with 30 degrees between each trace. Therefore, the strength observed in the megabin azimuth homogeneity plot versus the orthogonal version is due to more uniform statistical sampling.

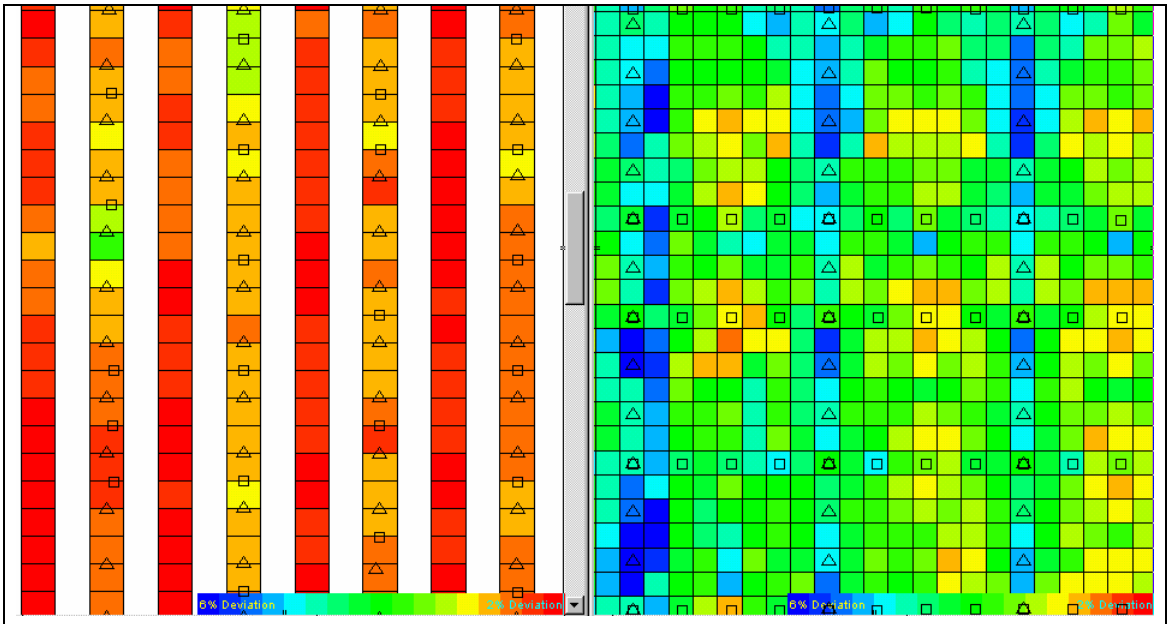

Figure 26
Booth versus Bentpath azimuth homogeneity.
Booth varies from 1.97 to 2.99 % standard deviation; Bentpath from 2.74 to 5.63 % standard deviation.

The accumulation of statistical analysis weighs heavily in favor of the megabin design. Because both source lines and receiver lines occupy the same physical line on the ground, the total linear kilometers to be permitted, produced, surveyed and travelled is less for the megabin versus the orthogonal. For the two surveys considered here, the megabin used 62 percent of the linear kilometers per square kilometer of surface coverage. The overall costs of the megabin survey (on a per square kilometer basis) were 20 to 30 percent lower than the orthogonal.

DATA COMPARISON OF CASE HISTORIES

Figure 27 is a grid map of the Bentpath East 3D as it was acquired. Note the extra effort involved in offsetting source segments around cultural features. Consider the additional amount of access trail and permit damages to be paid associated with servicing these offset locations.

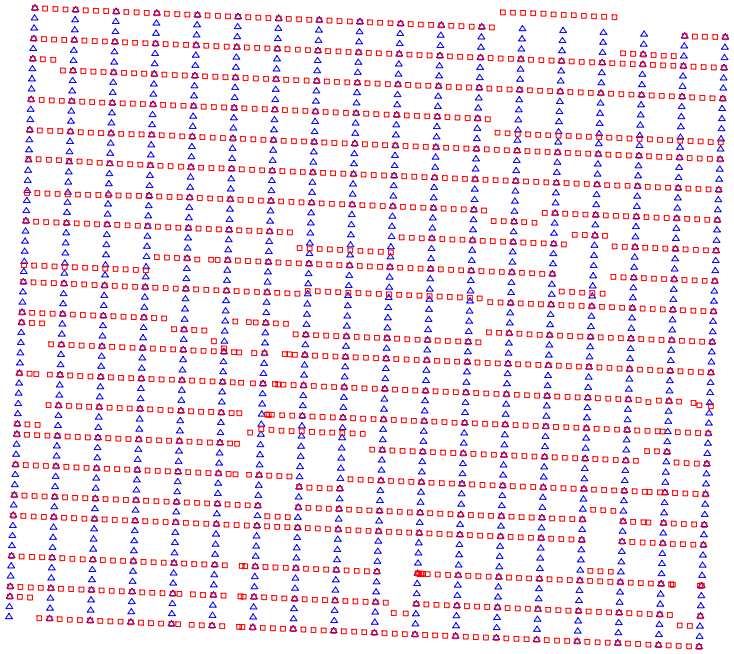

Figure 27
Bentpath East Orthogonal 3D grid as it was acquired.
Orthogonal 3D's require careful skidding and offsetting procedures to bypass cultural obstructions. This increases landowner costs and damages due to additional access. Offsetting often results in some confusion in locating shots during recording.

Figures 28 and 29 show time slices through the processed data volume from the Bentpath survey at 304 ms and 315 ms respectively. These reveal the crest and the base of a large reef. The reef is clearly imaged. The strong linear feature across the south boundary of the shallow slice is a result of major salt solution associated with the Dawn fault.

The time slices also illustrate the location of inline 65 (A-A') and crossline 64 (B-B'). These two data slices are reproduced in figures 30 and 31 respectively. Note the clear evidence of a large reef on these sections. Note, also the unstable nature of most reflections. See how many of the weak and moderate reflectors appear to alternate every few traces from stronger to weaker. This lack of consistency of character and amplitude is a result of a certain amount of geometric imprinting of the orthogonal geometry and its statistical deficiencies. This phenomenon also casts doubt on some of the character and amplitude changes observed in the time slices.

This feature was tested by two wells prior to the recording of the 3D. Since the interpretation of the 3D, three more wells have been drilled that confirm the interpretation.

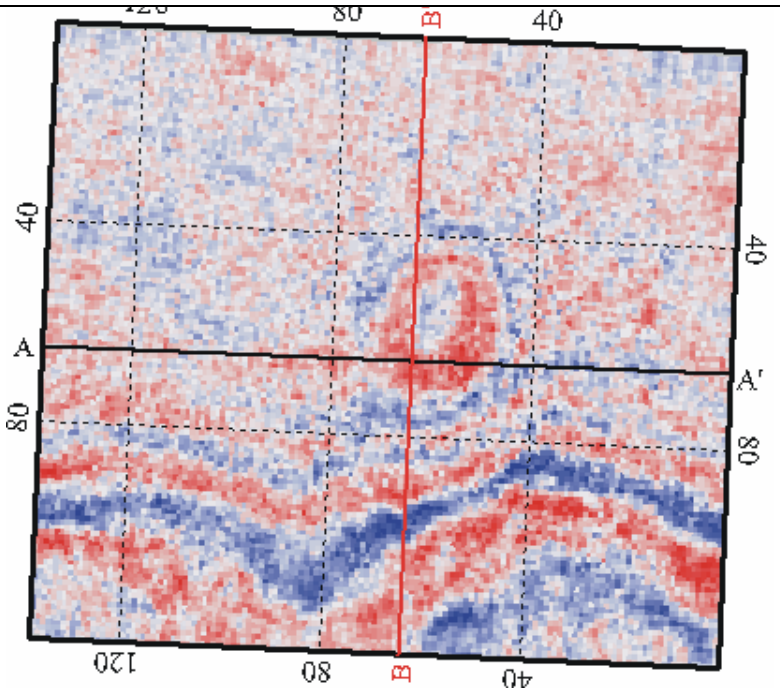

Figure 28
Bentpath East Orthogonal 3D timeslice at 304 ms.

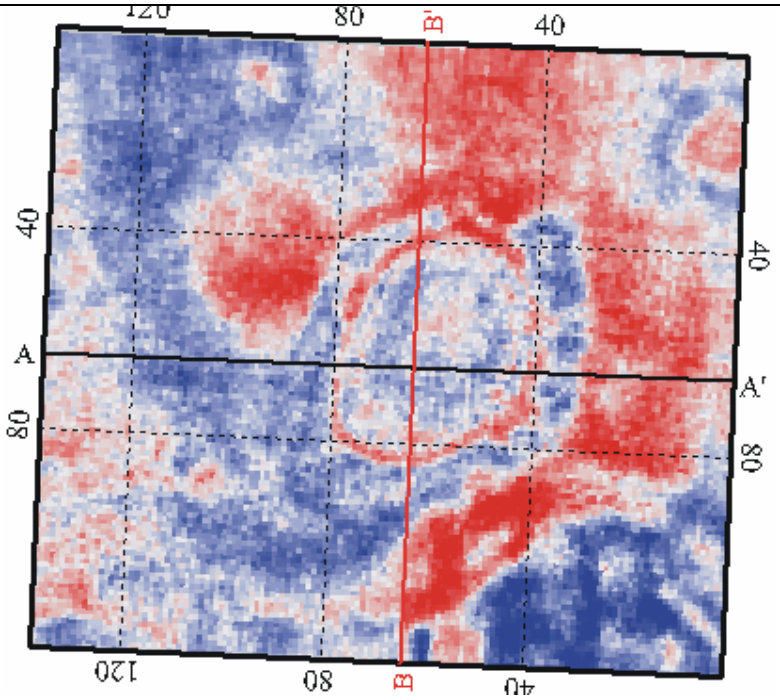

Figure 29
Bentpath East Orthogonal 3D timeslice at 315 ms.

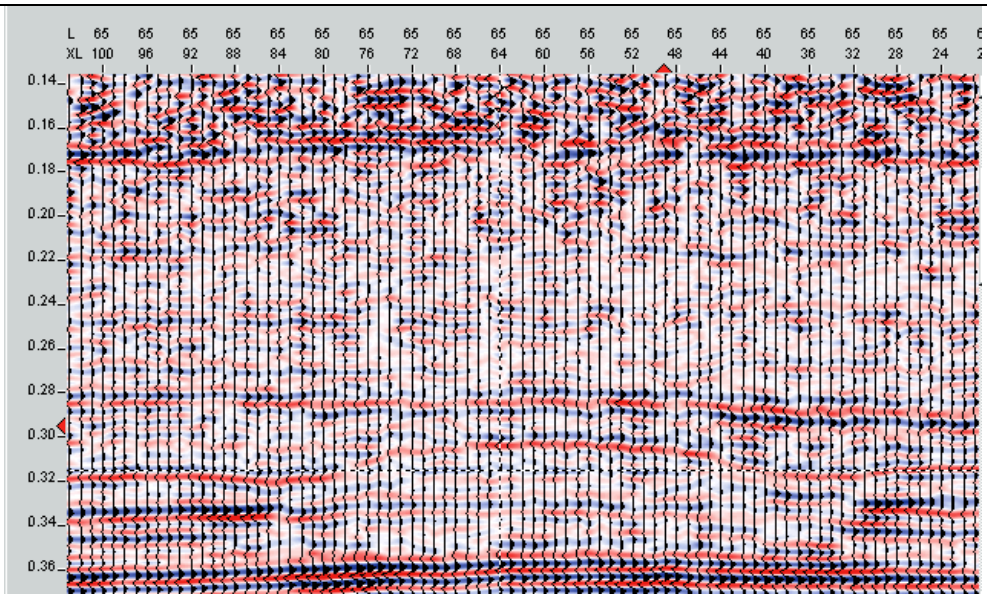

Figure 30
Bentpath East Orthogonal 3D inline 65.
.

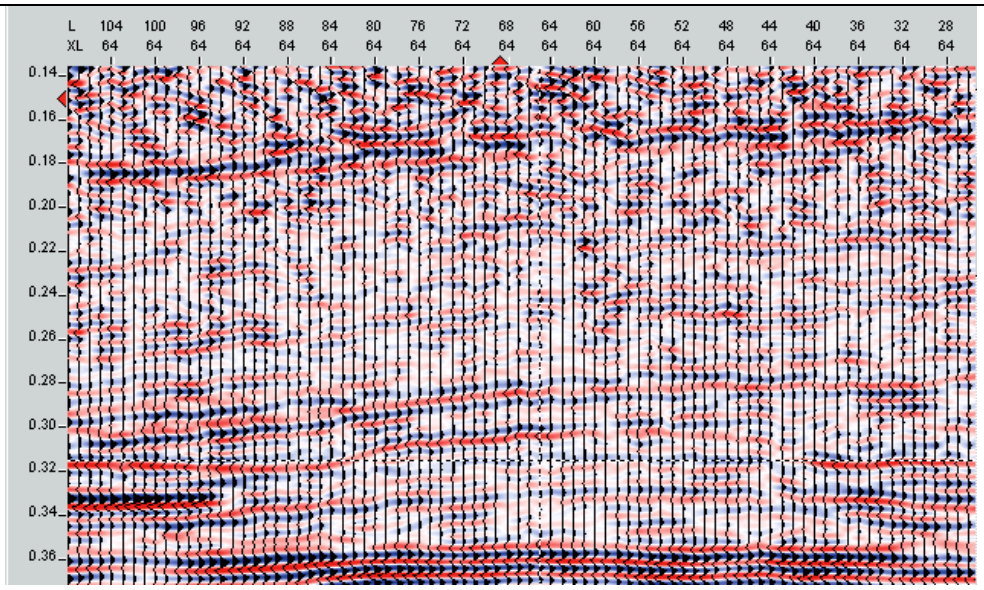

Figure 31
Bentpath East Orthogonal 3D crossline 64.
.

Figure 32 is a detail plot of the Booth Creek 3D grid as it was acquired. Notice that some shot points have been missed and others have been made up along existing lines at unused shot locations. Skidding and offsetting is not a difficult issue in a megabin design since we have already occupied at least half of the valid source locations. Usually, our fold is so high that we are not concerned about maintaining level of fold around gaps. Our greatest concern is to try to maintain optimal near offset contributions. Any shots located between existing lines would not compliment coverage in any of the modelled imaged bins. Therefore, such shots are not constructive additions to the program and we eliminate any additional access.

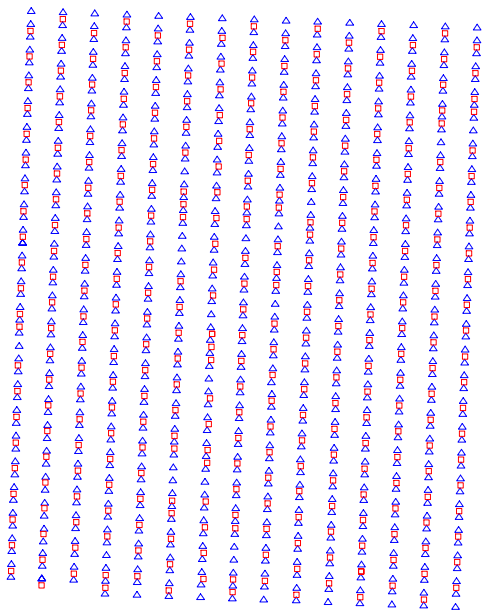

Figure 32
Booth Creek Megabin 3D grid as it was acquired.
Note there is no abnormal access to service make-up shots around cultural obstructions.

Figures 33 to 36 show a series of time slices from the Booth Creek 3D (356, 353, 348 and 332 ms). The development of a broad, low relief reef with a pinnacle crest is clearly evident. Unfortunately, these displays were created from a different work station with bolder colors and some edge smoothing. This makes the overall appearance different to the Bentpath time slices. However, note how small the Booth Creek pinnacle crest is. Less than 200 meters across, the rim of this feature contains two lobes, each only about 50 meters across. Yet the larger bins of the megabin design (and the interpolated traces) are clearly able to map this tiny detail. This is a testament to the image quality and statistical wavefield sampling inherent in the megabin method.

Figures 37 to 39 show some samples of the data slices through the crest of the reef (inline 46 and crossline 28 intersect over the crest) as well as near the edge of the low reef buildup (crossline 42). Note the general consistency of the reflection strength and character even in the shallow events (280 ms). There is no evidence of geometric imprinting in this data.

This prospect was tested in the low reef position by two wells prior to the recording of the 3D. There was no indication of the pinnacle. Since the interpretation of the 3D, two more reef crest wells have been drilled. The interpretation has been proven by the drill bit!

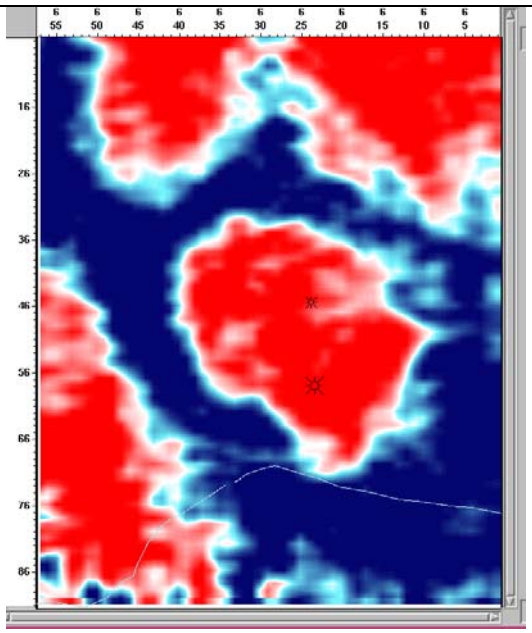

Figure 33
Booth Creek Megabin 3D time slice at 356 ms.

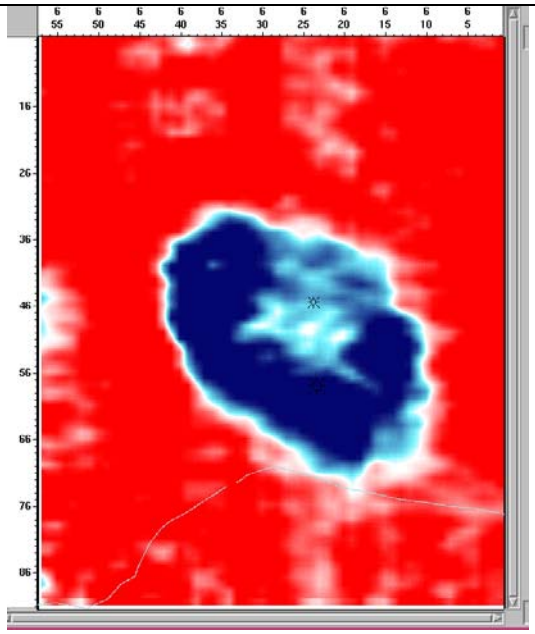

Figure 34
Booth Creek Megabin 3D time slice at 353 ms.

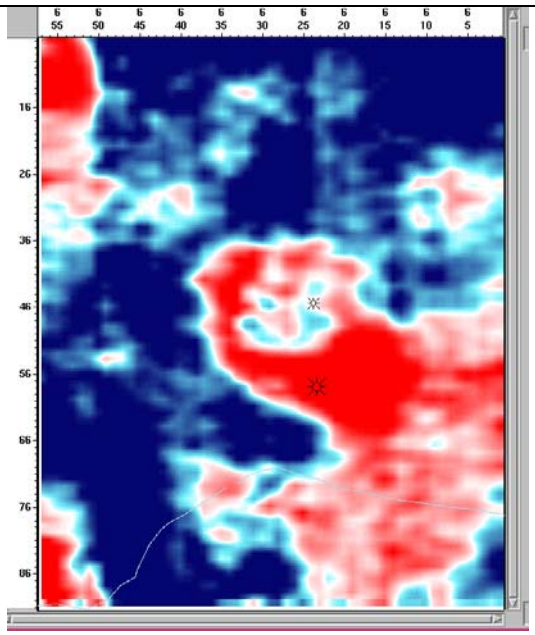

Figure 35
Booth Creek Megabin 3D time slice at 348 ms.

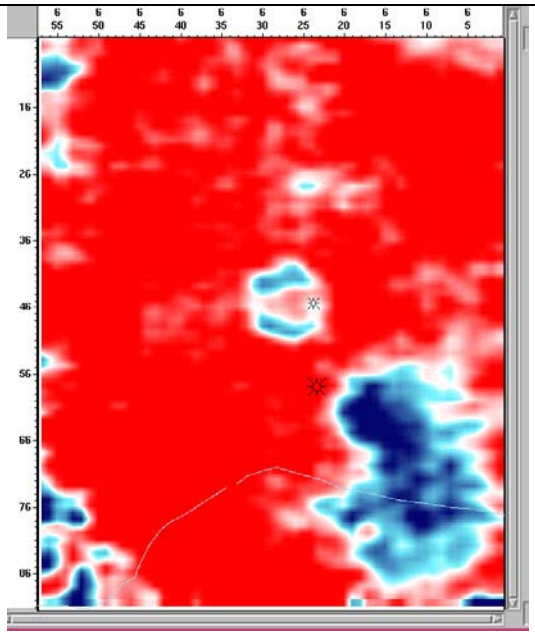

Figure 36
Booth Creek Megabin 3D time slice at 332 ms.

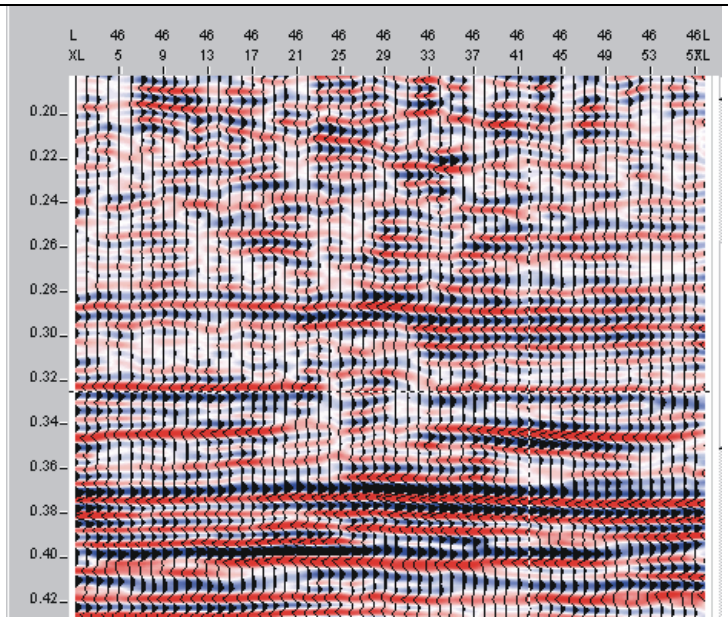

Figure 37
Booth Creek Megabin 3D inline 46.

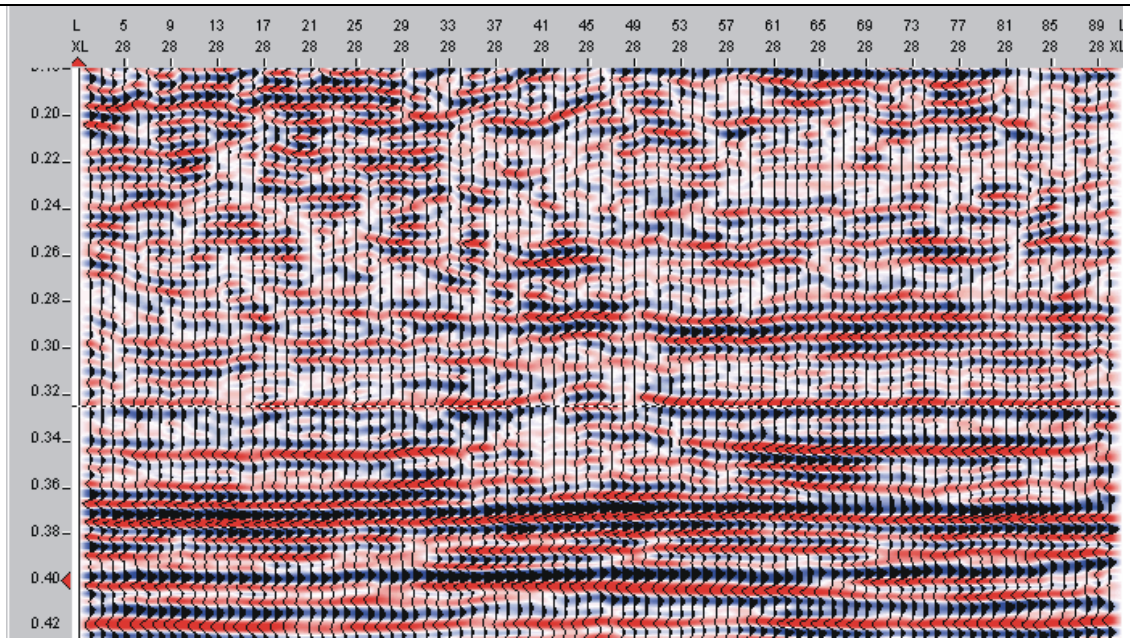

Figure 38
Booth Creek Megabin 3D crossline 28.

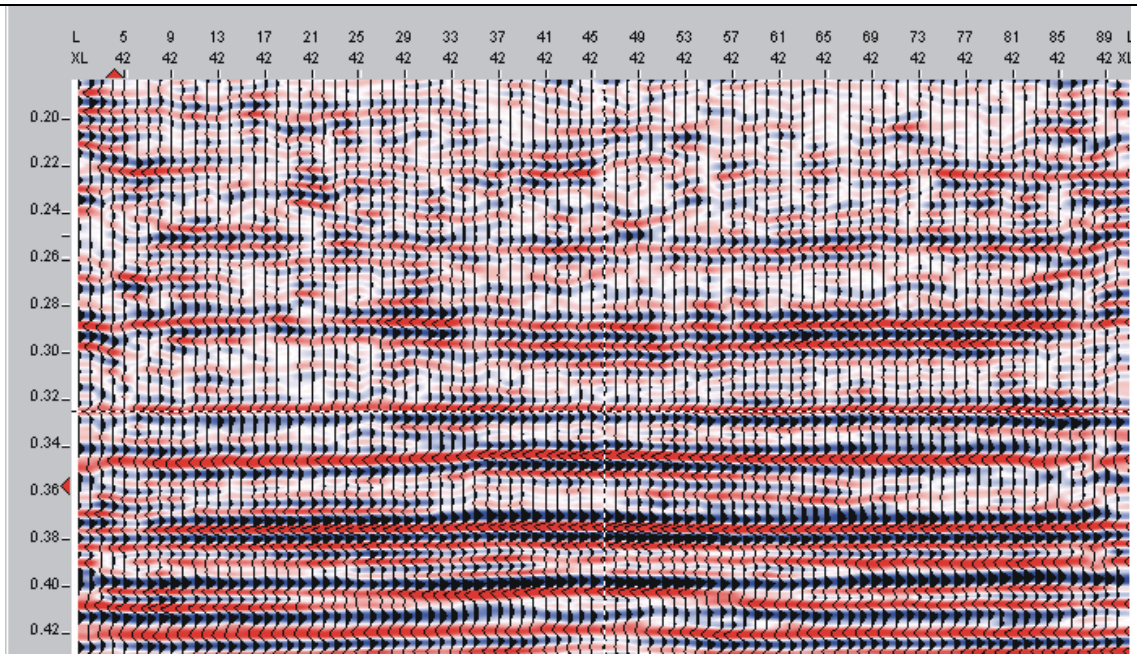

Figure 39
Booth Creek Megabin 3D crossline 42.

CONCLUSIONS

The megabin style of 3D was introduced to SW Ontario in 1998. Since then, many 3D programs of this style have been recorded. Cost savings of 20 to 30 percent over more conventional 3D programs have been realized. Landowner impact is greatly reduced and the task of permitting is made somewhat easier. These benefits alone would justify the method even if there was a slight deterioration of data quality. The fact is, the megabin technology provides better sampling statistics than recent conventional designs. The image quality is enhanced and stabilized. Interpretation is more reliable than it has ever been.

The megabin strategy works very well in the Michigan Basin, partly due to the shallow target depth. In much deeper basins, where longer source-receiver offsets are useful, the bin-driven design of the megabin becomes more costly compared to sparse, fold-driven designs. The image quality of megabin is the closest 3D equivalent of the 2D "stack array" strategy. It can provide the best wavefield sampling and deliver statistics valuable to the processor and interpreter. For prospects where long source-receiver offsets are available, the cost ratio of megabin to conventional design makes the megabin method difficult to defend. However, for shallower targets it represents the cheapest, lowest impact and best image quality of all options to the users of 3D methods.

ACKNOWLEDGMENTS

The authors would like to thank Union Gas Limited for sharing their data sets with the industry to promote better understanding of modern methods. They showed the courage and the insight to try new methods.

CanGeo Ltd. provided much input and helped adapt the megabin method to suit SW Ontario operational considerations.

We will always be indebted to Bill Goodway and Brent Ragan of PanCanadian Petroleums who developed and enhanced the megabin technology. Admirably, PanCanadian has chosen to openly share this technology with the industry. They have patented the method primarily as a defensive measure to protect it from patent by others. This gives them the control to keep the method open to all potential users.

REFERENCES

Goodway, Bill and Ragan, Brent, Personal Communication

Porsani, Milton J., September-October 1999. Seismic Trace Interpolation Using Half-Step Prediction Filters. Geophysics, volume 64, number 5, pages 1461-1467, Society of Exploration Geophysicists.

Spitz, S., June 1991. Seismic Trace Interpolation in the F-X Domain. Geophysics, volume 56, number 6, pages 785-794, Society of Exploration Geophysicists.